*Journal of Communications Technology, Electronics and Computer Science, Issue 11, 2017*
*ISSN 2457-905X*

# Harmonic Analysis of Switching Power Supply based on Conventional Triangulation Method

[1]Abdulkadir Iyyaka Audu and [2]Jibril Danladi Jiya
[1]Computer Engineering Department, University of Maiduguri, Nigeria
Mechatronic Engineering Department, Abubakar Tafawa Balewa University, Bauchi, Nigeria
[1]lm324fairchild@gmail.com, [2]jibjiya@yahoo.co.uk

***Abstract*—The advent of multilevel inverter topology has brought forth various pulse-width modulation (PWM) schemes as a means to control the switching of the active components in each of the multiple voltage levels in the inverter. In conventional triangulation, the carrier signal used in PWM is triangular in nature. In this paper, harmonic characterization of trapezoidal power supply (TPS) is carried out based on conventional triangulation method. TPS is a high frequency switching power supply system widely used in telecommunication companies. In multimedia distribution, hybrid fiber/coax (HFC) network dramatically connects optical fiber to the neighborhood with coax cable to the residence. Compared with all-fiber or all-coaxial networks, this network when powered with trapezoidal shaped voltage waveform allows for segmentation of services and high reliability, distribution efficiency, and low cost. Therefore, the analysis presented in this paper aims to emphasize that conventional triangulation method requires that the input dc voltage to the inverter system be made constant. When this condition is not satisfied, lower order harmonics and sub-harmonics which the output inductor-capacitor filter cannot remove are generated. Hence the efficient performance of TPS is affected.**

***Keywords—pulse-width modulation; harmonics; modulation index; switching frequency; trapezoidal voltage waveform***

## I. INTRODUCTION

In recent years, HFC distribution networks have emerged as one of the preferred approaches for distributing multimedia services to the customer, [1], [2], particularly by the cable TV industry. This hybrid dramatically network connects optical fiber to the neighborhood with coax cable to the residence. Compared with all-fiber or all-coaxial networks, this network allows for segmentation of services and high reliability, distribution efficiency, and low cost.

HFC networks require load voltage waveform which is trapezoidal. Additional requirements of high reliability and high input power factor demand that a study of the frequency spectrum of TPS be carried out. The strategic engagement of TPS system in optical/coax networks demands that harmonics analysis be made part of the performance indices of the TPS system itself. A typical control strategy of TPS is shown in fig. 1.

The need for reliability in power supplies used in the telecommunication industry has obviously been with us for many years. With the increased use of electrical power and our dependency on an electrical supply, reliability has become an increasing concern [2].

Typical assets such as valuable data, essential services and production process plants can be lost or seriously disturbed by power supply breaks or contamination. An uninterruptible power supply (UPS) can avoid potentially catastrophic havoc caused by electricity supply line disturbances.

Behind this protection, however, is the need for a sound UPS design based on a thorough specification to achieve reliable and consistent functioning. Reference [3] have it that in order to achieve bump less operation when the bypass switch is turned on, it is necessary to guarantee prior good synchronization between the inverter output voltage and the primary source voltage. The same is true when the transfer switch is engaged in offline or line-interactive UPS.

TPS has become an economic proposition for telecommunication industries where HFC networks are used [1].

Harmonic composition of the output of TPS is analyzed in this paper. Trapezoidal voltage waveform and its area of application are presented in introduction section I. An overview of harmonics and power electronics structure are discussed in the section II. Section III is devoted to harmonic analysis. Discussion on the generated harmonics is made in section IV. The conclusion about this paper is drawn in section V.

## II. OVERVIEW OF HARMONICS

PWM is synonymous with power electronics [4], [5], [6]. The competence of PWM is subject to the switching frequency, switching algorithm, switching devices, which constitute the inverter, and over-modulation [7]. Intrinsically, the process of PWM is always expected to generate either odd or even harmonics as a by-product [8], [9], [10]. The complex nature of the consequence of not having any of the subject factors appropriate is the simultaneous generation of both odd and even harmonics, and sub-harmonics, [11], [12], [13]. The load

filter of the UPS system is usually not in a position to cope with this type of situation [14]. Therefore, the power quality of the UPS system is significantly reduced and the following are affected [1]:

1) The input current is not in phase with the ac supply voltage (unity displacement factor is not achieved).

2) The input current presents a low-harmonic distortion.

3) Both features (1 and 2) result in a low overall input power factor.

Therefore, it becomes pertinent that we have a decent level of understanding which focuses on the frequency spectrum of a TPS system based on conventional triangulation method.

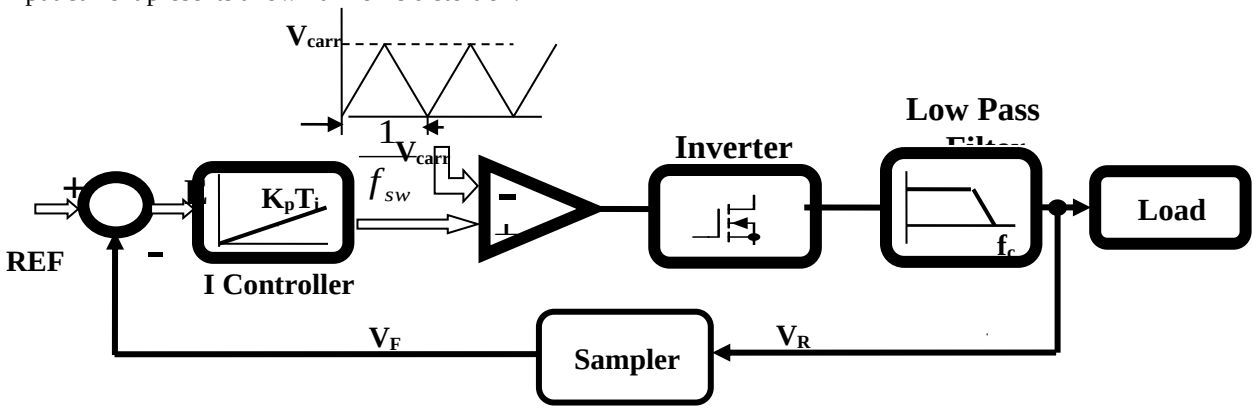


Fig. 1. Controlled block diagram of a trapezoidal UPS system

## III. Harmonics of a TPS Based on Conventional Triangulation Method

Consider the conventional carrier-based pulse width modulation as show in fig. 2. The width modulated pulses are produced at the output of the modulator by comparing a trapezoidal modulating waveform (reference) $\upsilon_m(t)$, which is to be syntheses, with a triangular carrier wave $\upsilon_c(t)$.

The trapezoidal modulating wave $\upsilon_m(t)$ can be written as

$$v_m(t) = A|\sin(\omega_o t)| \qquad 0 \le A \ge 1 \tag{1}$$

Where

$A$: Amplitude (or so called modulation index) of the reference wave

$\omega_o$: Inverter output frequency

Let $$B = \frac{\omega_c}{\omega_o} \tag{2}$$

Where $\omega_c/\omega_o$ is the ratio of the carrier frequency to the output frequency. Therefore, the triangular carrier wave $\upsilon_c(t)$ can be written as

$$v_{c(t)=\left|\frac{B}{\pi}\omega_o t - 2k\right|} \tag{3}$$

For $\frac{(2k-1)\pi}{B} \le \omega_o t \le \frac{(2k+1)}{B}$

Where k = 1, 2, 3, ……, B

If we let $F = {}^{B}/_{2} = {}^{\omega_c}/_{\omega_m}$ is the ratio of the carrier frequency to the modulating frequency, then it is seen that the $kth$ trough is positioned at

$$P_k = \frac{k\pi}{F} \tag{4}$$

This is true since (3) have slopes of $\pm\frac{B}{\pi}$

Let us denote the points of intersection of the carrier and modulating waves by $б_{2k-1}$ and $б_{2k}$ within the kth notch defined by

$$P_k - \left(\frac{\pi}{B}\right) \le \sigma_{2k-1} < \sigma_{2k} \le P_k + \left(\frac{\pi}{B}\right) \tag{5}$$

Then from (5) we can write

$$P_k - \left(\frac{\pi}{B}\right) \le \sigma_{2k-1}$$

$$\frac{k\pi}{F} - \left(\frac{\pi}{B}\right) \le \sigma_{2k-1}$$

$$\frac{2k\pi}{B} - \left(\frac{\pi}{B}\right) \le \sigma_{2k-1}$$

$$\pi(2k-1) \le B\sigma_{2k-1}$$

$$2k - \left(\frac{B\sigma_{2k-1}}{\pi}\right) \le 1 \tag{6}$$

Combining (1) and (6), we have

$$2k - \left(\frac{B\sigma_{2k-1}}{\pi}\right) = A|\sin\sigma_{2k-1}| \quad (7)$$

Similarly, from (5) we can write $\sigma_{2k} \leq P_k + {}^{\pi}/_{B}$ and when simplified further as in the previous part leads to

$$\left(\frac{B\sigma_{2k}}{\pi}\right) - 2k = A|\sin\sigma_{2k}| \quad (8)$$

Re-arranging (7) and (8), we will obtain

$$\sigma_{2k-1} = P_k - \frac{\pi A|\sin\sigma_{2k-1}|}{B} \quad (9)$$

$$\sigma_{2k} = P_k + \frac{\pi A|\sin\sigma_{2k-1}|}{B} \quad (10)$$

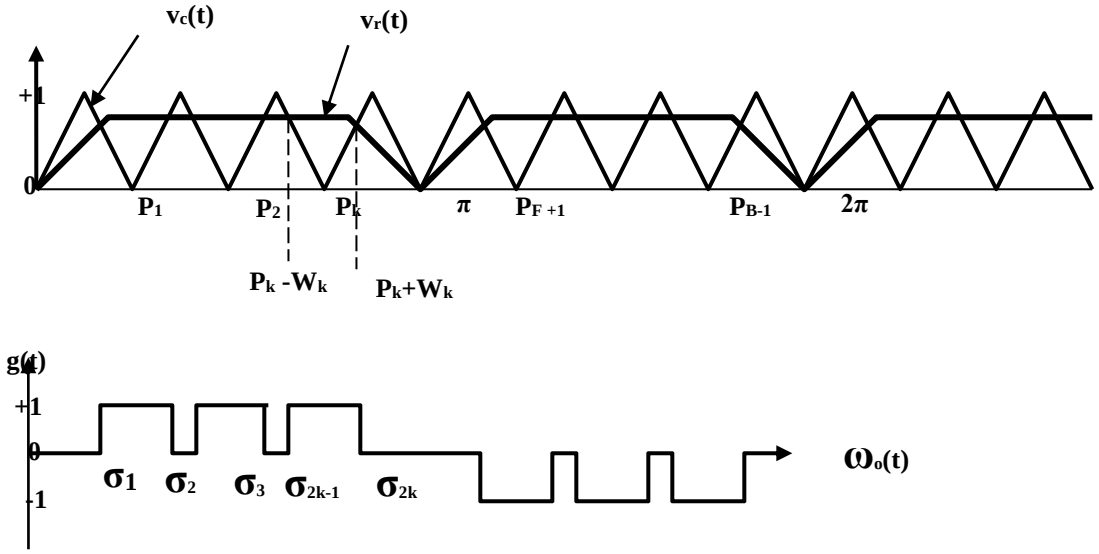


Fig. 2. The conventional triangulation method.

Numerical method is the most appropriate in solving (9) and (10) due to their transcendental and non-linear nature. For a situation where the carrier frequency is much greater than the modulating frequency, (1) can be written as

$$v_m(\omega_o t) \approx A|\sin P_k| \quad (11)$$

for $P_k - \frac{\pi}{B} < \omega_o t < P_k + \frac{\pi}{B}$ and $k = 1,2,\ldots,B$

Therefore, (9) and (10) simplify to

$$\sigma_{2k-1} \approx P_k - \frac{\pi A|\sin P_k|}{B} \quad (12)$$

$$\sigma_{2k-1} \approx P_k + \frac{\pi A|\sin P_k|}{B} \quad (13)$$

The half- width of the $kth$ pulse in the output wave could be obtained by subtracting (12) from (13), i.e

$$W_k = \frac{\sigma_{2k}-\sigma_{2k-1}}{2} \approx \frac{1}{2}\left\{\left(P_k + \frac{\pi A|\sin P_k|}{B}\right) - \left(P_k - \frac{\pi A|\sin P_k|}{B}\right)\right\} \quad (14)$$

$$W_k \approx \frac{\pi A|\sin P_k|}{B} \quad (15)$$

Therefore, (12) and (13) become

$$\sigma_{2k-1} \approx P_k - W_k \quad (16)$$

$$\sigma_{2k} \approx P_k + W_k \quad (17)$$

Equation (16) and (17) represent the intersections within the $kth$ notch. The transfer function g(t) of the inverter is defined as

$$g(t) = \frac{v_o(t)}{v_i(t)} = \begin{Bmatrix} +1, for\ \sigma_{2k-1} \leq \omega_o t \leq \sigma_{2k}\ and\ 1 \leq k \leq (F-1) \\ -1, for\ \sigma_{2k-1} \leq \omega_o t \leq \sigma_{2k}\ and\ (F+1) \leq k \leq (B-1) \\ 0, otherwise \end{Bmatrix} \quad (18)$$

In (18) the output voltage (unfiltered) and inverter input voltage are denoted by $v_o(t)$ and $v_i(t)$ respectively. In Fig. 2, it can be seen that the pulse train (having $B-2$ pulses per cycle) is an odd periodic function, therefore, the complex exponential form of Fourier series will be a good representation of the inverter switching (or transfer) function. i.e

$$g(t) = \sum_{n=-\infty}^{\infty} c_n exp(jn\omega_o t) \quad (19)$$

$c_n$ is defined as

$$c_n = -\frac{1}{jn\pi}\sum_{k=1}^{F-1}\{\cos(n\sigma_{2k}) - \cos n\sigma_{2k-1}\} \quad (20)$$

Substituting for $б_{2k-1}$ and $б_{2k}$ from (16) and (17) in (20), we have

$$c_n \approx -\frac{1}{jn\pi}\sum_{k=1}^{F-1}\{\cos(nP_k + nW_k) - \cos(nP_k - nW_k)\} \quad (21)$$

Using trigonometric identities, (21) becomes

$$c_n \approx 2\frac{1}{jn\pi}\sum_{k=1}^{F-1}\sin(nW_k)\sin(nP_k) \quad (22)$$

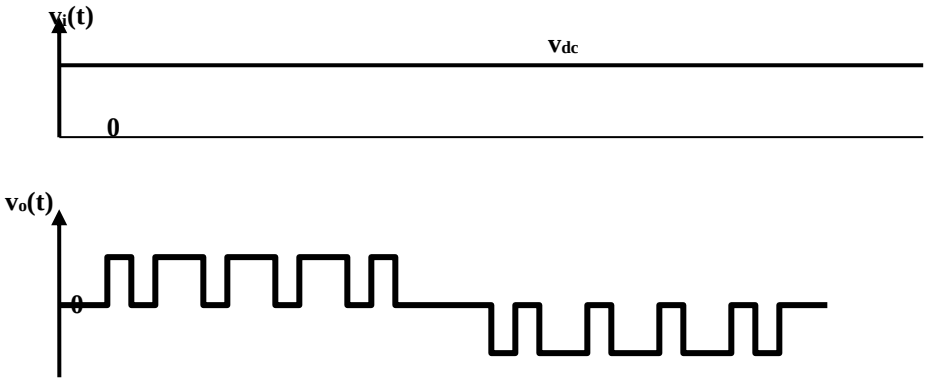


Fig. 3. Output voltage waveform for fixed input voltage

Where $W_k$ is expressed by (15). When n is very small compare with $B$ or $A$ far less than unity, then (23) becomes

$$\sin(nW_k) \approx \sin\left(\frac{nA\pi}{B}\sin P_k\right) \approx \sin\left(\frac{nA\pi}{B}\right)\sin P_k \quad (24)$$

Substituting (24) in (22), we get

$$c_n \approx \frac{1}{jn\pi}\sin\left(\frac{nA\pi}{B}\right)\left[\sum_{k=1}^{F-1} 2\sin(nP_k)\sin P_k\right] \approx \frac{1}{jn\pi}\sin\left(\frac{nA\pi}{B}\right)\left[\sum_{k=1}^{F-1}\cos\left(\frac{(n-1)k\pi}{F}\right) - \sum_{k-1}^{F-1}\cos\left(\frac{(n+1)k\pi}{F}\right)\right] \quad (25)$$

Therefore, further simplification yields

$$c_n \approx \begin{Bmatrix} 0, & for\ n \neq mB \pm 1\ and\ m = 0,1,2,\ldots. \\ \frac{F}{j(mB+1)\pi}\sin\left(\frac{(mB+1)A\pi}{B}\right), & for\ n = mB+1 \\ \frac{-F}{j(mB-1)\pi}\sin\left(\frac{(mB-1)A\pi}{B}\right), & for\ n = mB-1 \end{Bmatrix} \quad (26)$$

However,

$$\sin(nW_k) \approx \sin\left(\frac{nA\pi}{B}\sin P_k\right) \quad (23)$$

Substituting, $c_n$, from (26) in (18), we obtain the inverter switching function as

$$g(t) \approx \sum_{m=-\infty}^{\infty}\frac{F}{j(mB+1)\pi}\sin\left(\frac{(mB+1)A\pi}{B}\right)e^{[j(mB+1)\omega_o t]} - \sum_{m=-\infty}^{\infty}\frac{F}{j(mB-1)\pi}\sin\left(\frac{(mB-1)A\pi}{B}\right)e^{[j(mB-1)\omega_o t]} \quad (27)$$

If the inverter input voltage $v_i(t)$, is fixed (as shown in fig. 3) by sufficient filtering and equals

$$v_i(t) = v_{dc} \quad (28)$$

However, the output voltage of the inverter is given by

$$v_o(t) = g(t)v_i(t) \approx \sum_{m=-\infty}^{\infty}\frac{FV_{dc}}{j(mB+1)\pi}\sin\left(\frac{(mB+1)A\pi}{B}\right)e^{[j(mB+1)\omega_o t]} - \sum_{m=-\infty}^{\infty}\frac{FV_{dc}}{j(mB-1)\pi}\sin\left(\frac{(mB-1)A\pi}{B}\right)e^{[j(mB-1)\omega_o t]} \quad (29)$$

$$v_o(t) = g(t)v_i(t)$$
$$\approx \sum_{m=-\infty}^{\infty} \frac{FV_{dc}}{j(mB+1)\pi} \sin\left(\frac{(mB+1)A\pi}{B}\right) D_1$$
$$- \sum_{m=-\infty}^{\infty} \frac{FV_{dc}}{j(mB-1)\pi} \sin\left(\frac{(mB-1)A\pi}{B}\right) D_2$$

(30)

$$D_1 = 2j \sin(mB+1)\omega_o t - e^{-j(mB+1)\omega_o t}$$

$$D_2 = 2j \sin(mB-1)\omega_o t - e^{-j(mB-1)\omega_o t}$$

Further simplification yields

$$v_o(t)$$
$$= \left(\frac{BV_{dc}}{\pi} \sin\frac{A\pi}{B}\right) \sin\omega_o t$$
$$+ \sum_{m=1}^{\infty} \frac{BV_{dc}}{(mB+1)\pi} \left(\sin\frac{(mB+1)A\pi}{B}\right) (\sin(mB+1)\omega_o t)$$
$$- \sum_{m=1}^{\infty} \frac{BV_{dc}}{(mB-1)\pi} \left(\sin\frac{(mB-1)A\pi}{B}\right) (\sin(mB-1)\omega_o t)$$

(31)

When $v_o(t)$is applied to a second-order low pass filter, then the fundamental value $v_{of}(t)$, of $v_o(t)$ is obtained. This is because the predominant harmonics in (31) are the $(B \pm 1)$th. When the unwanted higher order harmonics are filtered get

$$v_{of}(t) \approx \left(\frac{BV_{dc}}{\pi} \sin\frac{A\pi}{B}\right) \sin\omega_o t$$

(32)

When $B$ is quite large compared with $A$, then

$$\sin\frac{A\pi}{B} \approx \frac{A\pi}{B}$$

Therefore, eqn (32) becomes

$$v_{of}(t) \approx AV_{dc} \sin\omega_o t$$

(33)

Therefore, it can be concluded that the fundamental value of $v_{of}(t)$ is almost linearly proportional to the value of $A$ is dependent on inverter input voltage $V_{dc}$ which is the constant of proportionality.

When the input voltage at the DC bus of an inverter fluctuates due to insufficient filtering, it can be expressed as

$$v_i(t) = \sum_{n=-\infty}^{\infty} h_n e^{jn\omega_i t}$$

(34)

Where $\omega_i$ is the input fluctuation frequency and

$$h_n = \frac{1}{2\pi} \int_0^{2\pi} v_i(t) e^{-jn\omega_i t} h(\omega_i t)$$

(35)

Combining eqns. (30) and (35), we get

$$v_o(t)$$
$$= \sum_{m=-\infty}^{\infty} \sum_{m=-\infty}^{\infty} \frac{Fh_n}{j(mB+1)\pi} \left(\sin\frac{(mB+1)A\pi}{B}\right) D_3$$
$$- \sum_{m=-\infty}^{\infty} \sum_{m=-\infty}^{\infty} \frac{Fh_n}{j(mB-1)\pi} \left(\sin\frac{(mB-1)A\pi}{B}\right) D_4$$

(36)

$$D_3 = e^{j[(mB+1)\omega_o + n\omega_i]t}$$

$$D_4 = e^{j[(mB-1)\omega_o + n\omega_i]t}$$

## IV. Discussion

Equation (36) depicts that conventional triangulation method does not allow for effective utilization of the supply voltage. This is because the modulation index, m cannot have a practical value of more than 0.68 ($0 \leq A \leq 1$, theoretically).

One other importance of this analysis is that it has highlighted the problem of input dc voltage variation, that is, if the constant of proportionality was not constant. This situation is expressed in eqn. (34), it is obvious that the unfiltered output voltage contains large amounts of lower order harmonics and sub-harmonics, especially the harmonics of frequencies $|\omega_i \pm \omega_o|$ and hence the required volt-ampere rating of output filter for this case is higher than for the case of fixed inverter input voltage. However, if the constant of proportionality was constant then higher order harmonics would be generated and these can be easily filtered.

## V. Results

The waveforms of Fig. 4(a) through to (j) are related to the synchronization and reference unit. The transient waveform of Fig. 1(a) represents the sampled 50Hz mains voltage. This is fed into a zero-level comparator which produces a square wave at the same frequency as shown in Fig. 4(b). This signal serves as an input to a phase-locked loop (PLL) configured as a multiplier. The PLL yields a square wave of 51.2 KHz shown in Fig. 4(c). This is then passed through an edge detector in which the waveform of Fig. 4(d) is obtained. This signal feeds the CMOS switch which is positioned parallel to the capacitor of the integrator which constitutes the carrier generator. Waveforms of Figs. 4(e), (g), (i) are obtained from the 12-stage counter (4040), positioned along the feedback path of the PLL and represent the address signals for the 74LS151 multiplexers. The waveforms of Fig 4(f) and (h) are consequently generated from the multiplexers. These signals in turn control the integrator which generates the trapezoidal reference signal of Fig. 4 (j). The trapezoidal output load voltage is generated

from H-bridge inverted topology using the control signals of Fig. 4

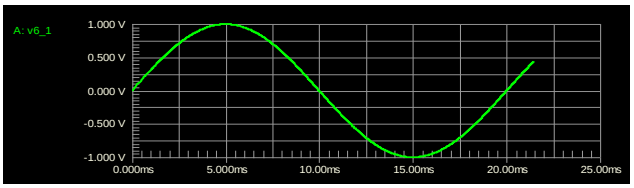


(a)

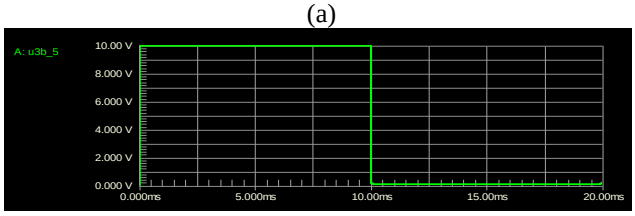


(b)

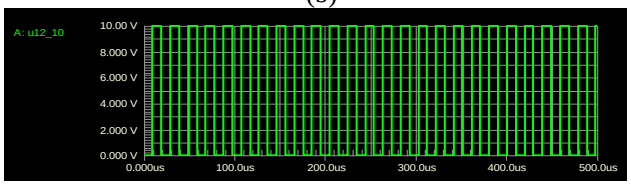


(c)

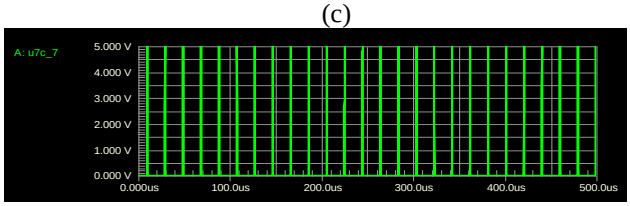


(d)

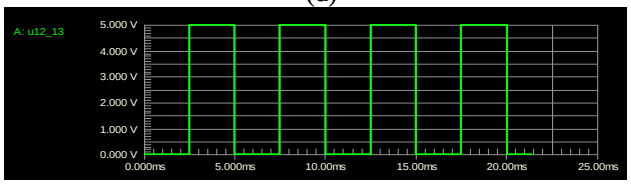


(e)

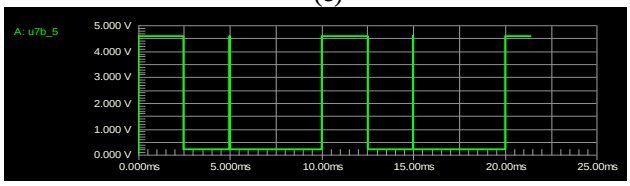


(f)

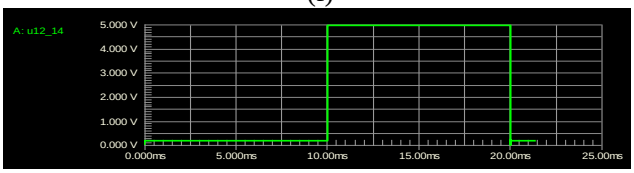


(g)

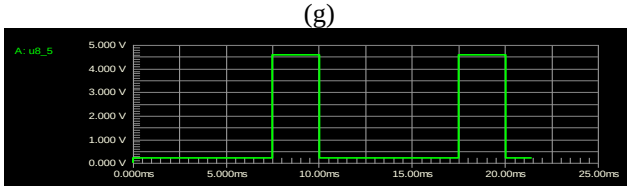


(h)

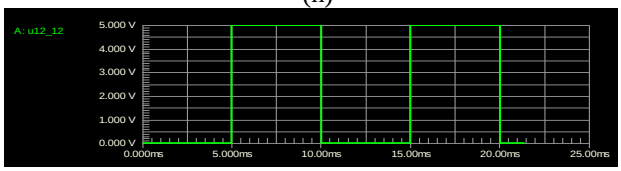


(i)

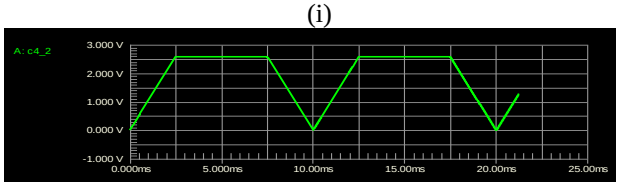


(j)

Fig. 4. Transient waveforms of reference and synchronization unit.

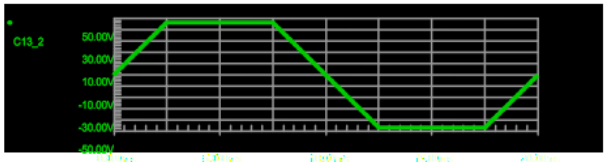


Fig. 5. Trapezoidal output voltage.

## VI. Conclusions

In this study, the frequency characterization of TPS based on conventional triangulation method has been presented. The study drives at the fact that the switching frequency must be high in order to keep the switching losses low. Also, the fundamental output voltage of TPS is almost linearly proportional to the modulation index, where the constant of proportionality is the dc voltage input voltage.

In the implementation, the input dc voltage is made higher compared to the expected output alternating trapezoidal voltage of 90V peak-to-peak.

When it becomes extremely difficult to keep the input dc voltage constant, then the fluctuating input voltage method will need to be used in the generation of trapezoidal voltage load waveform.

## REFERENCES

[1] P. K. Jain, J. R. Espinoza and H. Jin, "Performance of a single-stage ups system for single-phase trapezoidal-shaped ac-voltage supplies," IEEE Transactions on Power Electronics, Vol. 13, No. 5, pp. 912-92, 1998.

[2] M. Qiu, P. K. Jain and H. Jin, "Modeling and performance of a power distribution system for hybrid fiber/coax networks," IEEE Transactions on Power Electronics, Vol. 14, No. 2, pp. 273-281, 1999.

[3] R. M. Santos Filho, P. F. Seixas, P. C. Cortizo, L. A. Torres and A. F. Souza, "Comparison of three single-phase PLL algorithms for UPS applications," IEEE Transactions on Industrial Electronics, Vol. 55, No. 8, pp. 2923-2932, 2008.

[4] J. Platts and J. St. Aubyn, Uninterruptible power supplies. Peter Peregrinus Ltd, London, 1992.

[5] Y. Tzou, S. Jung and H. Yeh, "Adaptive repetitive control of pwm inverter for very low thd ac-voltage regulation with unknown loads," IEEE Transactions on Power Electronics, Vol. 14, No. 5, pp. 973-981, 1999.

[6] G. Moschopoulos, and P. Jain, "Single-phase single-stage power-factor-corrected converter topologies," IEEE Transactions on Industrial Electronics," Vol. 52, No. 1, pp. 23-35, 2005.

[7] Z. J. Zhou, X. Zhang, P. Xu, and W. X. Shen, "Single-phase uninterruptible power supply based on Z-source inverter," IEEE Transactions on Industrial Electronics, Vol. 55, No. 8, pp.2997-3004, 2008.

[8] A. M. Trzynadlowski and S. Legowski, "Minimum-loss vector pwm strategy for three-phase inverters," IEEE Transactions on Power Electronics, Vol. 9, No. 1, pp. 26-34, 1994.

[9] A. M. Have, R. J. Kerkman and T. A. Lipo, "Carrier-based pwm overmodulation strategies: analysis, comparison, and design," IEEE Transactions on Power Electronics, Vol. 13, No. 4, pp. 674-685, 1998.

[10] A. M. Have, R. J. Kerkman, and T. A. Lipo, "Simple analytical and graphical methods for carrier-based pwm-vsi drives," IEEE Transactions on Power Electronics, Vol. 14, No. 1, pp. 49-61, 1999.

[11] B. Zhao, Q. Song, W. Liu, and Y. Xiao. "Next-generation multi-functional modular intelligent UPS system for smart grid," IEEE Transactions on Industrial Electronics, Vol. 60, No. 9, pp. 3602-3618, 2013.

[12] Z. Lining, Evaluation and dsp based implementation of pwm approaches for single-phase dc-ac converters, M. Eng. Thesis on Power Electronics, (Unpublished), Famu-Fsu College of Engineering, The Florida State University, USA, 2005.

[13] D. Lee and G. Lee, "A novel overmodulation technique for space-vector pwm inverter," IEEE Transaction. on Power Electronics, Vol. 13, No. 6, pp 1145-1151, 1998.

[14] I. A. Khan and R. W. Erickson, "Systhesiss and analysis of harmonic-free three-phase inverters," IEEE Trans. on Power Electronics, Vol. 9, No. 6, pp. 567-579, 1994.